Volume 7 | Number 19 | 7 October 2020

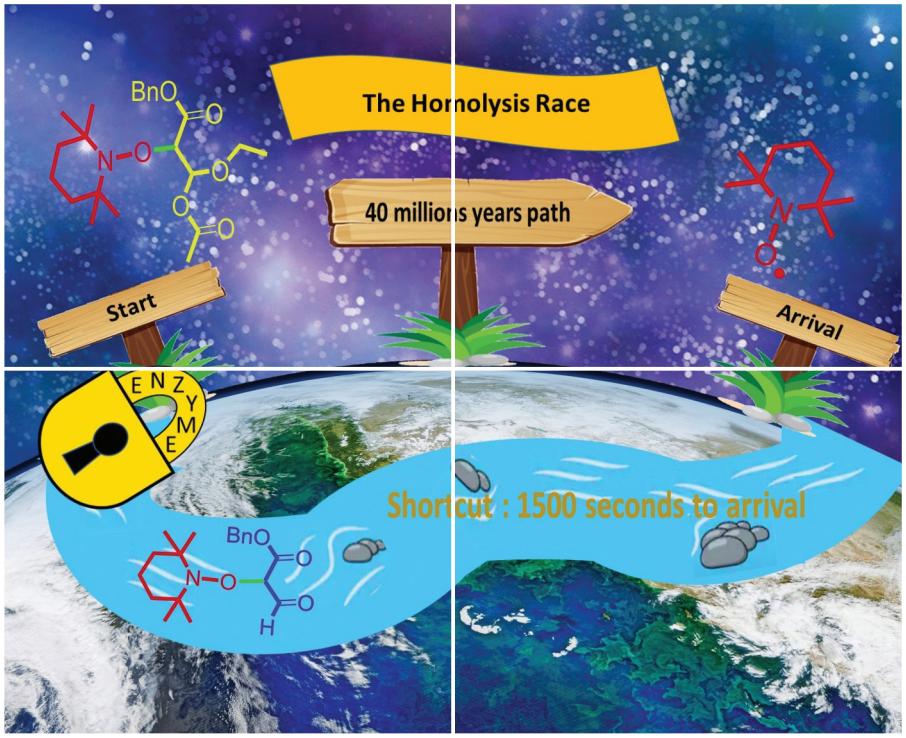

ORGANIC CHEMISTRY

FRONTIERS

CCS 中国化学会 CHINESE CHEMICAL SOCIETY
SIOC 1950
ROYAL SOCIETY OF CHEMISTRY
rsc.li/frontiers-organic

ORGANIC CHEMISTRY FRONTIERS

RESEARCH ARTICLE

View Article Online
View Journal | View Issue

Check for updates

Cite this: *Org. Chem. Front.*, 2020, **7**, 2916

An enzymatic acetal/hemiacetal conversion for the physiological temperature activation of the alkoxyamine C–ON bond homolysis†

Muriel Albalat,[a] Gérard Audran,*[b] Maxence Holzritter,[b] Sylvain R. A. Marque,*[b] Philippe Mellet,*[c,d] Nicolas Vanthuyne[a] and Pierre Voisin[d]

Received 9th May 2020,
Accepted 21st July 2020

DOI: 10.1039/d0qo00559b

rsc.li/frontiers-organic

The potential of alkoxyamines as theranostic agents has been recently promoted by our groups. The success of such an approach relies on the switch upon enzymatic triggering between highly stable precursor alkoxyamines and activated alkoxyamines exhibiting fast homolysis of the C–ON bond. Hence, at 37 °C in water, benzyl 2-(2,2,6,6-tetramethylpiperidin-*N*-oxy)-3-ethoxy-3-acetoxypropanoate and benzyl 2-di*tert*-butylaminoxy-3-ethoxy-3-acetoxy propanoate afford t_{max} of 2000 s (35% conversion) and 500 s (60% conversion), respectively, for the C–ON bond homolysis in the presence of Subtilisin A whereas $t_{1/2}$ of *ca.* 42 thousand millenniums and 330 years are expected accordingly to E_a values in *n*-propanol. These results nicely highlight the *on*/*off* switch, provided that an enzymatic activity controls the C–ON bond homolysis.

Open Access Article. Published on 30 July 2020. Downloaded on 7/29/2025 12:37:41 PM.
This article is licensed under a Creative Commons Attribution-NonCommercial 3.0 Unported Licence.

Introduction

Labile alkoxyamines were first[1–4] applied, in 1986, as controller/initiator agents for Nitroxide Mediated Polymerization (NMP).[5–11] During the last decade, several variants – Enhanced Spin Capture Polymerization (ESCP),[12] Nitroxide Mediated PhotoPolymerization (NMP2),[13–15] Coordination Initiated-NMP (CI-NMP),[16] Surface Initiated-NMP (SI-NMP),[17] Spin Label NMP (SL-NMP),[18,19] Plasmon Initiated NMP (PI-NMP)[20] – have emerged, which extend the versatility of this radical polymerization technique. Recently, the lability of the C–ON bond has been used to develop new applications of alkoxyamines, *e.g.*, self-healing polymers,[21,22] dynamic microcrystal assemblies,[23] and information-encoding polymers.[24–26] For a few years,[27] our groups have promoted the therapeutic application of alkoxyamines as drugs against cancer.[28–30] For such an application, we aim to combine four antagonistic features: a highly stable precursor (or pro-drug), a highly reactive drug, random reactivity, and specific addressing. The aim is to circumvent drug-resistant cancer by using highly reactive and unselective drugs, and to improve the patient welfare by using highly selective pro-drugs *via* specific addressing, which is a step towards personalized medicine. For several years, a keen interest in using radical species (mainly ROS) as drugs has been observed,[31] although two challenges have arisen: the bio-distribution of the drug and the generation of radicals at physiological temperature. Radical generation at physiological temperature has been mainly achieved by radiochemistry and by PDT, with the use of photosensitizers. Nevertheless, it has a strong impact on the welfare of the patient and it is not always efficient. A few years ago,[27] we proposed the concept of smart alkoxyamines, *i.e.*, stable alkoxyamines that are transformed into labile alkoxyamines upon chemical triggering. Several chemical activation events – protonation,[32] alkylation,[33,34] oxidation,[33,34] coordination[35,36] – have been applied to both nitroxyl and alkyl fragments.[37–39] To overcome the aforementioned bottlenecks, the specific addressing and activation events are ensured by the persistent and specific activities of protease present in the tumor environment, thus highly labile alkoxyamines in the vicinity of tumors are released.[27,40] Hence, the proteases must hydrolyze specific peptides to release highly reactive alkyl radicals in a handful of seconds to react in the vicinity of the tumor, *i.e.*, the issues of drug bio-distribution and release location are circumvented. Recently, we reported the triggering of the C–ON bond homolysis due to

[a]*Aix-Marseille Univ, CNRS, Centrale Marseille ISM2 Marseille, France*
[b]*Aix-Marseille Univ, CNRS, ICR case 551, Avenue Escadrille Normandie-Niemen, 13397 Marseille Cedex 20, France. E-mail: g.audran@univ-amu.fr, sylvain.marque@univ-amu.fr*
[c]*INSERM, 33076 Bordeaux Cedex, France. E-mail: philippe.mellet@rmbs.u-bordeaux.fr*
[d]*Centre de Résonance Magnétique des Systèmes Biologiques, UMR 5536 CNRS, Case 93, University of Bordeaux 146 rue Leo Saignat, 33076 Bordeaux Cedex, France. E-mail: philippe.mellet@rmsb.u-bordeaux.fr*

†Electronic supplementary information (ESI) available: Experimental procedures, analysis data, kinetics, LFER analysis and XRD data are reported as ESI. CCDC 1989155. For ESI and crystallographic data in CIF or other electronic format see DOI: 10.1039/d0qo00559b

This journal is © the Partner Organisations 2020

Open Access Article. Published on 30 July 2020. Downloaded on 7/29/2025 12:37:41 PM.
This article is licensed under a Creative Commons Attribution-NonCommercial 3.0 Unported Licence.

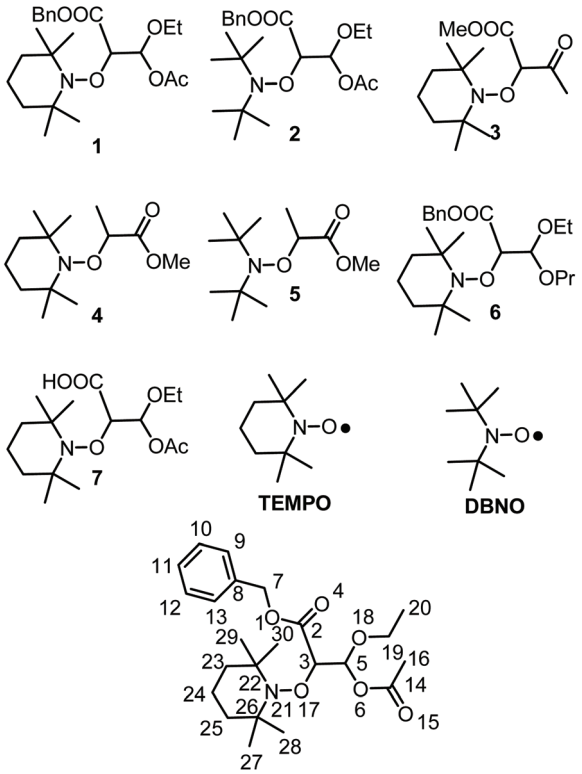

Chart 1 Alkoxyamines and nitroxides discussed in the article.

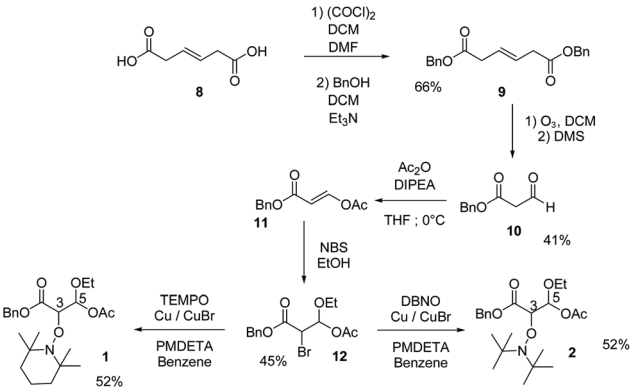

Scheme 1 Preparation of **1** and **2** (see ESI†).

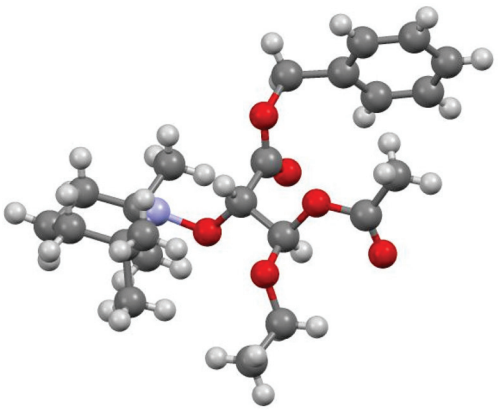

Fig. 1 XRD structure (see ESI†) of ***3S5R*-1** aka **1A(−)**.

specific enzymatic activity but the large half-life time $t_{1/2}$ of 111 min observed at 37 °C and the insufficient stability of the pro-drug impeded any application of alkoxyamines as drug.[40] Consequently, our research is now focused on the development of switches able to transform a stable alkoxyamine into a highly labile alkoxyamine upon specific enzymatic activity.

To this end, alkoxyamines **1** and **2** (Chart 1) carrying a malonic-like alkyl fragment with a carbonyl function hidden as an unsymmetrical acetal were prepared and investigated in various conditions of temperatures, solvents, and enzymes. Using Subtilisin A as trigger, $t_{1/2}$ values of a few hundred seconds were observed for **1** and **2**, whereas several centuries are expected in the absence of activation.

Results

Synthesis of 1 and 2

With the adapted reported procedure, *trans*-beta-hydromucanic acid **8** was esterified with benzyl alcohol to yield **9**,[41] which was oxidized by ozonolysis to afford **10**. The enolate of **10** was scavenged by acetic anhydride to yield the *E*-enol **11**. The ethanol solution of **11** in the presence of NBS (generation of an intermediate bromonium) afforded bromoacetal **12**.[42] Using the ATRA procedure, in the presence of **TEMPO** and **DBNO**,[43] bromide **12** yielded alkoxyamines **1** and **2**, respectively (Scheme 1 and ESI†).

Because of the presence of stereocenters in the alkyl fragment, two diastereoisomers are observed for **1** and **2**. Taking into account that enzymes are dramatically sensitive to the configuration of the stereocenters, enantiomers were separated by chiral HPLC (see ESI†).

Isomers were noted **A** and **B**, and (+) and (−) signs were given according to chromatographic retention order and to the deviation of the polarized light, respectively. Colourless crystal plates of enantiomer **1A(−)**‡ were obtained from diethyl ether (slow evaporation at 4 °C) and provided configurations *S* and *R* (Fig. 1) for carbon atoms 3 and 5, respectively (Fig. 1 and Chart 1). The geometrical parameters of **1A(−)** were not very different from those reported for similar models (alkoxyamines carrying an ester group) except for shorter O17–C3 bond and N21···C3 distance by 0.02 Å and 0.01 Å, respectively. Hence, configurations 3*S*5*R* and 3*R*5*S* are ascribed to isomers **1A(−)** and **1A(+)**, respectively, and the relative configuration RR/SS to isomers **1B(+)** and **1B(−)**. As no XRD data are available for **2**, the assessment of absolute and/or relative configurations is not possible.

‡CCDC 1989155.

Open Access Article. Published on 30 July 2020. Downloaded on 7/29/2025 12:37:41 PM.
This article is licensed under a Creative Commons Attribution-NonCommercial 3.0 Unported Licence.

Table 1 Homolysis rate constants k'_d at different temperatures T, in various conditions, and the subsequent activation energies E_a as well as the re-estimated k_d values at 120 °C and the half-life time $t_{1/2}$ at 37 °C

		Conditions	T (°C)[a]	k_d (s^{-1})[b]	E_a (kJ mol^{-1})[c]	k_d (120 °C, s^{-1})	$t_{1/2}$ (37 °C, year)[d]
1	A+[e]	*t*-BuPh	164	6.0×10^{-4}	147.3	8.0×10^{-6}	433
	A−[e]	*t*-BuPh	163	8.3×10^{-4}	146.0	1.1×10^{-5}	294
	B+[e]	*t*-BuPh	155	3.3×10^{-4}	146.5	9.3×10^{-6}	371
	B−[e]	*t*-BuPh	164	3.7×10^{-4}	149.2	1.0×10^{-5}	353
	[f,g]	*n*-PrOH	85	4.4×10^{-10}	162.6	6.0×10^{-8}	231 000
	A+[h]	*n*-PrOH/H_2O:2/8	96	4.8×10^{-11}	174.0	1.8×10^{-9}	18.5×10^6
	A−[h]	*n*-PrOH/H_2O:2/8	96	2.8×10^{-11}	176.0	9.9×10^{-10}	41.5×10^6
	B−[h]	*n*-PrOH/H_2O:2/8	96	5.9×10^{-11}	173.4	2.2×10^{-9}	14.7×10^6
	B+[h]	*n*-PrOH/H_2O:2/8	96	7.5×10^{-11}	172.0	3.4×10^{-9}	8.5×10^6
2	A+[i]	*t*-BuPh	100.6	1.5×10^{-5}	137.4	1.3×10^{-4}	13
	A−[i]	*t*-BuPh	100.7	1.9×10^{-5}	136.6	1.7×10^{-4}	9
	B+[i]	*t*-BuPh	101.9	2.0×10^{-5}	138.6	9.2×10^{-5}	20
	B−[i]	*t*-BuPh	101.5	1.8×10^{-5}	137.2	1.4×10^{-4}	12
	[f,g]	*n*-PrOH	70.2	1.6×10^{-8}	145.8	1.0×10^{-5}	330
	[f,g]	*n*-PrOH	89.5	2.8×10^{-7}	145.4	1.2×10^{-5}	281
3		*t*-BuPh[j]	[k]	[k]	139.3	7.3×10^{-5}	27
		Water/MeOH[j]	[k]	[k]	121.6	0.016	248 hours
4		*t*-BuPh[l]	[k]	[k]	141.8	3.4×10^{-5}	72
5		*t*-BuPh[l]	[k]	[k]	128.2	0.002	133 days
6	[e]	*t*-BuPh	158	5.8×10^{-4}	145.8	1.1×10^{-5}	296

[a] Error is ±1 °C. [b] Error <5%. [c] Activation energies E_a were estimated using a frequency factor A of 2.4×10^{14} s^{-1}, as reported in ref. 9. Errors in E_a are around 1–2 kJ mol^{-1}. [d] Unless otherwise mentioned. [e] k_d values determined using eqn (1). [f] 4 isomer mixture. [g] k_d values determined using eqn (2) and $[alkoxyamine]_0 = 0.1$ M. [h] k_d values determined using eqn (2) and $[alkoxyamine]_0 = 10^{-4}$ M. [i] k_d values determined using eqn (2) and $[alkoxyamine]_0 \approx 10^{-2}$ M. [j] See ref. 45. [k] Not given. [l] See ref. 53.

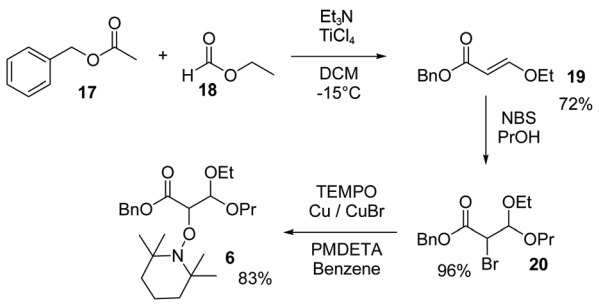

Scheme 2 Preparation of **6** (see ESI†).

Synthesis of 6

The enol **19** was synthesised by a condensation of benzyl acetate **17** and ethyl formate **18** activated by $TiCl_4$ as reported.[44] Propanol solution of **19** in the presence of NBS afforded bromoacetal **20**.[42] Using ATRA procedure,[43] in the presence of TEMPO, bromide **20** yielded alkoxyamine **6** (see Scheme 2 and ESI†).

Enzyme-free kinetics

Kinetics of **1** and **2** were measured as previously reported,[45] using either the plateau method (eqn (1), $[nitroxide]_\infty = [alkoxyamine]_0$) or the initial slope method (eqn (2), $[nitroxide]_\infty = [alkoxyamine]_0$). The homolysis of all the isomers was investigated in *t*-BuPh and in *n*-PrOH. Taking into account the high E_a observed in *t*-BuPh, *n*-PrOH (bp = 97 °C) was selected as solvent to mimic water as much as possible.

$$\ln\left(\frac{[nitroxide]_\infty - [nitroxide]_t}{[nitroxide]_\infty}\right) = -k'_d \times t \quad (1)$$

$$\frac{[nitroxide]_t}{[nitroxide]_\infty} = k'_d \times t \quad (2)$$

As expected, the pairs of enantiomers display the same values of k_d (Table 1) and the small differences in E_a between diastereoisomers are in the range (1–2 kJ mol^{-1}) of those already reported in the literature and do not deserve more comments.[46]

Using linear free energy relationships reported in the literature,[47,48] E_a of **1**§ and **2**¶ are estimated as 137.0 kJ mol^{-1} and 126.5 kJ mol^{-1},[45] respectively. Polar, steric, stabilization and conformational effects of the nitroxyl fragment **TEMPO** and **DBNO** in **1** and **2** are the same as those reported in the literature, as E_a of **2** is *ca.* 10 kJ mol^{-1} lower than E_a of **1**. On the other hand, E_a for **1** and **2** are clearly higher by 10 kJ mol^{-1} than expected from the literature,[46] denoting an unexpected effect (see Discussion), as parameters used to describe steric, polar, and stabilization effects in the alkyl fragment are rather reliable (see ESI†). The clear increase in E_a of **1** and **2** due to solvent effects, *i.e.*, by 15 kJ mol^{-1} (*ca.* 200-fold) and 8 kJ mol^{-1} (*ca.* 10-fold) from *t*-BuPh to *n*-PrOH, respectively, is in sharp

§ For **1**: $\sigma_{RS} = 0.18$, $\sigma_I = 0.16$ and $\upsilon = 0.83$. More details are provided in ESI.†
¶ For **2**, E_a is given by applying the increment −10.5 kJ mol^{-1} to E_a of **1**. See ref. 53.

This journal is © the Partner Organisations 2020

Open Access Article. Published on 30 July 2020. Downloaded on 7/29/2025 12:37:41 PM.
This article is licensed under a Creative Commons Attribution-NonCommercial 3.0 Unported Licence.

contrast to the slight decrease in E_a reported when changing from non-polar to polar solvents.[49,50] As claimed in a previous article,[45] this striking solvent effect is likely due to a change in conformation in the alkyl fragment depending on the dipole moment of the molecule, which is strongly sensitive to the solvation cage related both to the polarity and the structuredness/stiffness of the molecules of solvent. This is nicely supported by the 30-fold decrease in k_d of **1** from bulk *n*-PrOH to 2 : 8 *n*-PrOH : water (Table 1).

Enzymatic kinetics

Since an acetyl leaving group is not a favoured substrate for this enzyme, *i.e.*, the Michaelis constant K_m is very large, very high concentrations up to 6×10^{-3} M of the enzyme were used to afford the fast activation of the alkoxyamines. Fig. 2 and 3 display two groups of isomers: a fast reacting one (Fig. 2) and a slow reacting one (Fig. 3).

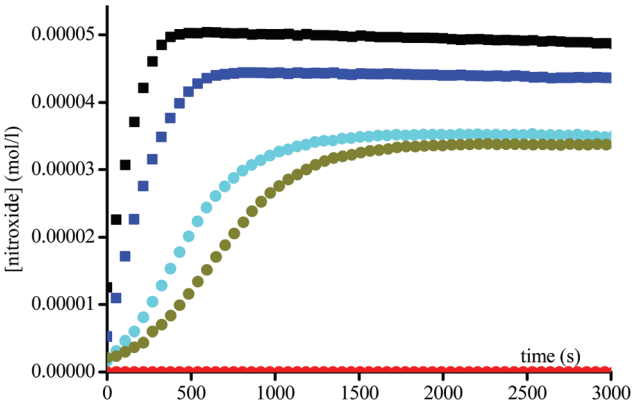

Fig. 2 Growth of TEMPO and DBNO released by the homolysis of **1A(–)** (●), **1B(+)** (●), **2A(–)** (■), and **2B(+)** (■) against time at 37 °C in buffer (pH = 7.4) and in the presence of Subtilisin A (1.5×10^{-3} M), and of **1A(–)** (●) in the absence of Subtilisin A. Initial concentrations in alkoxyamines are 0.1 mM.

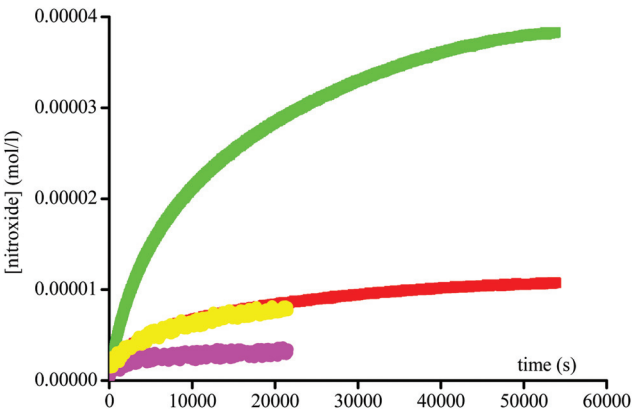

Fig. 3 Growth of **TEMPO** and **DBNO** released by the homolysis of **1A(+)** (●), **1B(–)** (●), **2A(+)** (■), and **2B(–)** (■) against time at 37 °C in buffer (pH = 7.4) and in the presence of Subtilisin A (1.5×10^{-3} M). Initial concentration in alkoxyamines are 0.1 mM.

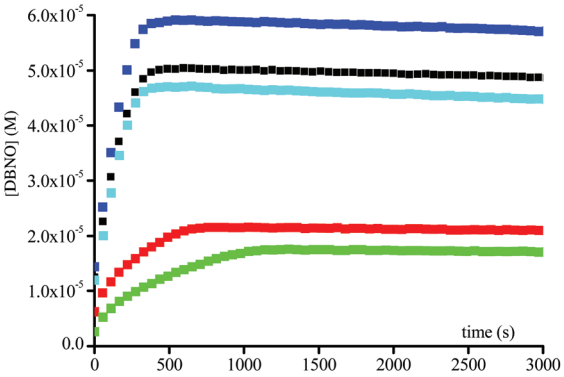

Fig. 4 Plots of **DBNO** released during the homolysis of 0.1 mM of **2A(–)** *vs.* time in buffer (pH = 7.42) at 37 °C and in the presence of various amounts of Subtilisin A (■) 4.0×10^{-4} M, (■) 8.3×10^{-4} M, (■) 1.6×10^{-3} M, (■) 3.3×10^{-3} M, and (■) 6.6×10^{-3} M.

Interestingly, two isomers of **1** and two isomers of **2** are present in each group, suggesting an enantiomeric selection by the enzyme. In the absence of enzyme no homolysis events were detected.

By varying the enzyme concentration, an optimum is observed around 3×10^{-3} M, affording the fastest homolysis rate and the highest conversion (Fig. 4). Surprisingly, for all enantiomers the maximal conversion for **1** and **2** is of 40% and 50%, respectively, and not the full conversion as expected. Furthermore the conversion varies with the enzyme concentration (Fig. 4).

In fact, Subtilisin A contains some residues, *e.g.*, cysteine or tyrosine residues, capable of reducing the nitroxide, as highlighted in Fig. 5, impeding the increase in concentration of the nitroxide up to completion. This loss of nitroxide is only clearly detected at high concentrations of the enzyme. Thus, when using Subtilisin A in large excess,‖ the values of k_5 are determined as $k_5^T = 3.0 \times 10^{-6}$ s^{-1} for **TEMPO** and $k_5^D = 1.1 \times 10^{-5}$ s^{-1} for **DBNO**,** assuming a pseudo first-order reaction to occur between the enzyme and the nitroxide, as shown in Scheme 3 and given by eqn (3).

Because the kinetics of enzymatically catalyzed reactions are often complicated,[51] because the enzyme plays both the role of catalyst and reducing agent for the nitroxide, because intermediates have not yet been clearly identified, the kinetic equations derived from Scheme 3 cannot be developed in a simple way and would not provide more information on the homolysis process.

$$k_5^{TorD} = k'[E] \quad (3)$$

‖ Values of k_4 are given to a factor depending on the number of cysteine and tyrosine on the enzyme.

** For **DBNO** alone, $k_5 = 5.3\ 10^{-7}$ s^{-1}.

Open Access Article. Published on 30 July 2020. Downloaded on 7/29/2025 12:37:41 PM.
This article is licensed under a Creative Commons Attribution-NonCommercial 3.0 Unported Licence.

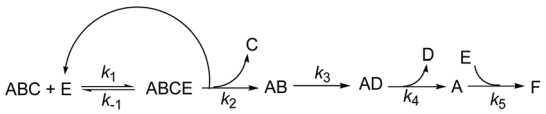

Scheme 3 Kinetic scheme for the decay of alkoxyamine **ABC** in the presence of enzyme **E** (Subtilisin A). **ABCE** is the enzymatic complex, **AB** the hemiacetal alkoxyamine (see Scheme 4), **AD** the activated aldehyde alkoxyamine (see Scheme 4), **A** and **D** the nitroxyl and alkyl radicals, respectively, and F the degradation product of the reaction between **A** and **E**.

Discussion

Alkoxyamines **1** and **2** exhibit E_a values (Table 1) in the range of those of their simple models **4** and **5**,[52] respectively, meaning that, as reported in literature,[46] conventional polar, steric and stabilization effects are ruling the C–ON bond homolysis. These differences of 5–10 kJ mol^{-1} in E_a are ascribed to a homoanomeric and hyperconjugation effects stabilizing the starting materials. As mentioned above, the conventional geometrical parameters of **1A(−)** are very close to those reported for ester based alkoxyamines,[48] except that alkoxyamines carrying acetal groups have never been reported. Interestingly, the dihedral angle <O17C3C5O6> exhibits a value of 180°, meaning that the two C–O bonds have an antiperiplanar conformation, favouring the hyperconjugation effect (Fig. 1 and 6). Thus, the donations from the oxygen lone pairs n_O of atoms O6 and O17 into the antibonding orbitals σ^* of O17–C3 and C5–O6 bonds, respectively, occur and this is known as the Plough effect.[53]†† Moreover, combination of the presence of electron withdrawing ester function at C2 and the dihedral angle <N21O17C3C2> close to 90° (Fig. 6) support the hyperconjugation interaction $n_{p,O} \rightarrow \sigma^*_{C3-C2}$ *via* the electron donation from p pure lone pair of O18 into the antibonding orbital of the C2–C3 bond The anomeric (hyperconjugation) effect,[54] intramolecular H-bonding[55] and intramolecular coordination[56] between the alkyl and nitroxyl fragments are well known for stabilizing starting materials and leading to stronger C–ON bond, *i.e.*, in all cases it is like cleaving an extra bond.

Indeed, the Plough effect due to the $n_{O17} \rightarrow \sigma^*_{C5-O18}$ interaction affords an interaction between the nitroxyl fragment with O17 and the alkyl fragment with C5–O18 bond, which may be considered as an extra weak bond to be cleaved for homolysis to occur. It is assumed that these comments hold for all other isomers of **1** (as well as for the isomers of **2**), as they exhibit very similar E_a that of **1A(−)**.

Although Subtilisin A (4.0×10^{-4} to 6.6×10^{-3} M) is not used in sub-stœchiometric amounts as expected in enzymatic catalysis, it still plays the role of a catalyst, as in its absence no homolysis occurs whereas in its presence a maximal apparent conversion of 50% and 30% (Fig. 2–4) is reached for **2A(−)** and **1A(−)**, respectively, in less than 500 s and 1500 s, respectively. Remarkably, less than 10^{-16} M of **1** and **2** are decomposed during this time in the absence of enzyme according to their E_a values! The dramatic effect of Subtilisin A on the stability of **1** and **2** is accounted for only by a dramatic change in structures of **1** and **2**. Indeed, the Subtilisin A enzyme is known as a poorly selective protease capable of hydrolyzing an ester bond, the acetoxy group in **1** and in **2** is thus "readily" hydrolysed (Scheme 4) to afford hemiacetal **13** and **14**, respectively. The latter are not stable in aqueous media and collapse into aldehydes **15** and **16** respectively, which are prone to homolyze into the corresponding **TEMPO** and **DBNO** and the malonic-like alkyl radicals (Scheme 4). This sequence of events is supported by the high values of E_a for **6** (E_a = 145 kJ mol^{-1}, Table 1) and **7** (E_a = 146 kJ mol^{-1}),[47]‡‡ which leads to discard the replacement of the acetoxy group of **1** by the propyloxy group in **6** and the hydrolysis of the benzyloxycarbonyl moiety of **1** into the carboxylic/carboxylate function in **7**.

Moreover, as **3** experiences a dramatic solvent effect from *t*BuPh to water/MeOH with a decrease in the E_a by 18 kJ mol^{-1},

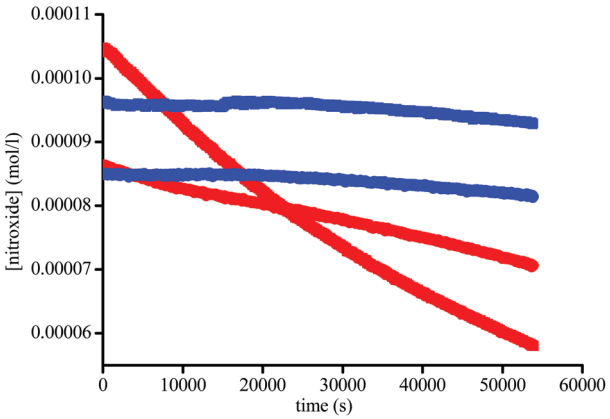

Fig. 5 Plot of [**1**] (●) and [**2**] (■) *vs.* time in the absence (blue) and in the presence of 1.5×10^{-3} M of Subtilisin A (red) at 37 °C in buffer (pH = 7.4).

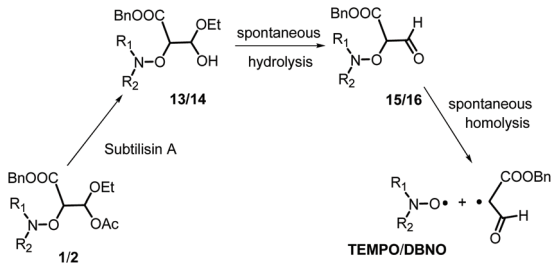

Scheme 4 Tentative activation pathway for the homolysis of **1** and **2** induced by Subtilisin A.

†† The difference between Plough effect and W effect lies in the position of the donating lone pair which is parallel to the bond onto which donating and accepting group are attached.

‡‡ Private communication of authors. Data for **6** will be reported in a forthcoming article.

This journal is © the Partner Organisations 2020

Open Access Article. Published on 30 July 2020. Downloaded on 7/29/2025 12:37:41 PM.
This article is licensed under a Creative Commons Attribution-NonCommercial 3.0 Unported Licence.

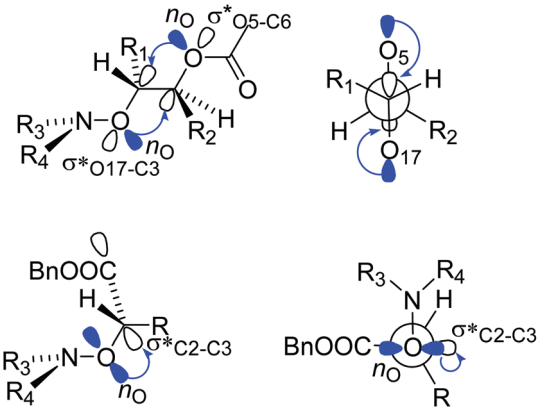

Fig. 6 Homoanomeric Plough (top) and hyperconjugation (bottom) effects in alkoxyamines **1** and **2**.

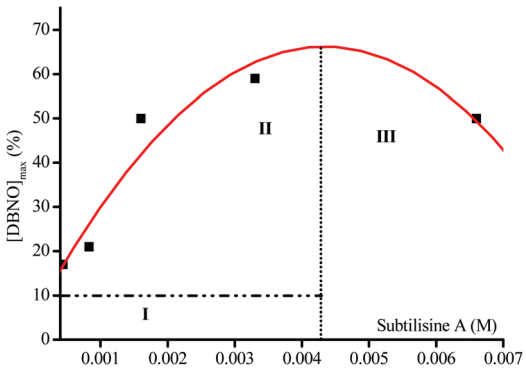

Fig. 7 Maximal concentration in **DBNO** (%) for various amounts of Subtilisin A.

the same effect is expected for **15**, with a conformational effect likely stronger, as the oxo group in **3** is replaced by a formyl group in **13**, which may favour the required conformation at TS, and hence, afford a striking increase in k_d. Therefore, the enzymatic hydrolysis of **1** affords the hemiacetal which is spontaneously hydrolized into formyl-based alkoxyamine **15**, which accounts for the spontaneous generation of **TEMPO**.††,§§¶¶ Unfortunately, despite several attempts it was not possible to prepare **13** *via* conventional methods, meaning either the formyl derivative **9** is less stable than the oxo derivative **3** or the intermediates do not react as expected. It is assumed that these comments hold for **2**.

Because of a side-reaction between nitroxides and Subtilisin A (Fig. 6 and Scheme 3) and a selective efficiency of the enzyme for the hydrolysis of the acetoxy group, the steady state in the nitroxide is reached between 5% to 50% conversion (Fig. 2 and 3). Indeed, for **1** and **2**, Subtilisin A shows a selectivity in favour of enantiomers **A(−)** and **B(+)** against enantiomers **A(+)** and **B(−)**. Taking into account that **1** and **2** exhibit very different homolysis rate constants and that **TEMPO** and **DBNO** react at different rates with Subtilisin A, the role of the nitroxyl fragment on the selectivity of Subtilisin A is unclear.

As mentioned above, in enzymatic catalysis, the use of a large excess of enzyme is rather unconventional. The rate of **DBNO** generation and the yield of the reaction vary with the enzyme concentration (Fig. 4), suggesting that for such a simple acetoxy leaving group the enzymatic activation is rate-limiting. The bell-shaped curve of the maximal concentration in nitroxide *vs.* the amount of Subtilisin A (Fig. 7) shows a maximal concentration of *ca.* 70% conversion in nitroxide for *ca.* 4 10^{-3} M in enzyme. Interestingly, this bell-shaped curve is divided in 3 regions: region I for sub-stœchiometric enzyme concentrations, for which a different regime (Fig. 7) is observed for the generation of nitroxide, because the non-reversible nitroxide and enzyme reaction competes with the enzyme-intermediate formation (ABCE in Scheme 3), affording lower and lower concentrations in enzyme with time, slowing down the formation of intermediate and, hence, the release of **15** and **16**; region II for an excess of enzyme for which the Ostwald assumption holds, and then the release of nitroxide is favoured over its degradation by the enzyme; and region III for which the excess of enzyme is so large that the decay of nitroxide by reaction with the enzyme becomes the favoured reaction.

Conclusions

The enzyme-triggered hydrolysis of acetal into hemiacetal, which, in turn, hydrolyzes spontaneously into aldehyde, is a powerful switch to transform highly stable alkoxyamines into highly labile ones. The results reported here show that the enzymatic reaction is the limiting event, in sharp contrast to

§§The occurrence of a charged intermediate during the enzymatic hydrolysis cannot be straightforwardly disregarded as it would dramatically increase the C–ON bond homolysis rate.

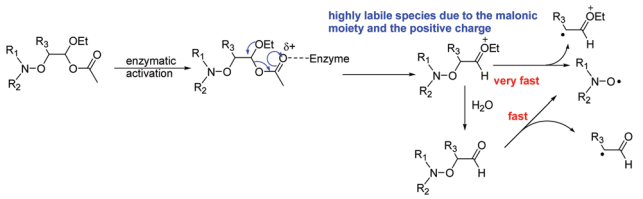

¶¶A reviewer mentioned the possible formation of enol which would dramatically favoured the N–O bond homolysis over the C–O bond homolysis. However, this possibility is discarded because using model **3** and several homologues (ref. 45), basic catalysis with various bases, *e.g.*, KH, LiH, NaH, HMDS, OH^-, and acidic catalysis, *e.g.*, H^+, Lewis acids and several traps, the formation of enol was never observed and starting materials always recovered.

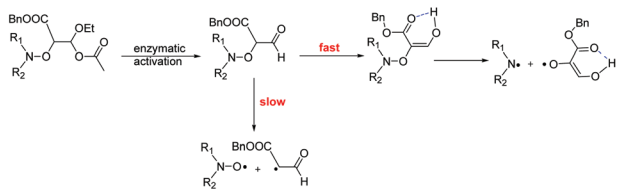

Open Access Article. Published on 30 July 2020. Downloaded on 7/29/2025 12:37:41 PM.
This article is licensed under a Creative Commons Attribution-NonCommercial 3.0 Unported Licence.

the results reported for an alkoxyamine locked with a peptide. Thus, the next step should focused on more targeted peptides including those relevant for the enzymes found in the tumour environment. Despite this limitation, more than 60% conversion of **2A(−)** is reached in less than 10 minutes, meaning that the homolysis of peptide-locked alkoxyamines should be faster, and that the C–ON bond can be weakened by changing the nitroxyl fragment, ester and alkoxy functions on the alkyl fragment.

Conflicts of interest

There are no conflicts to declare.

Acknowledgements

S. R. A. M., G. A., M. H., N. V., and M. A. are grateful to Aix-Marseille University and CNRS for support. P. M. and V. P. are grateful to University of Bordeaux and INSERM for support. S. R. A. M. and G. A., thank ANR for financial support (ANR-17-CE18-0017). All authors are grateful to Spectropôle (AMU/CNRS) platform for technical support.

Notes and references

1 D. H. Solomon, E. Rizzardo and P. Cacioli, *Eur. Pat. Appl.*, 1985, 135280; D. H. Solomon, E. Rizzardo and P. Cacioli, *US Pat*, 4,581,429, 1986; D. H. Solomon, E. Rizzardo and P. Cacioli, *Chem. Abstr.*, 1985, **102**, 221335q.

2 E. Rizzardo, Living free radical polymerisation, *Chem. Aust.*, 1987, **54**, 32–33.

3 C. H. J. Johnson, G. Moad, D. H. Solomon, T. H. Spurling and D. J. Vearing, The Application of Supercomputers in Modeling Chemical Reaction Kinetics: Kinetic Simulation of "Quasi-Living" Radical Polymerization, *Aust. J. Chem.*, 1990, **43**, 1215–1230.

4 G. Moad and E. Rizzardo, Alkoxyamine-Initiated Living Radical Polymerization: Factors Affecting Alkoxyamine Homolysis Rates, *Macromolecules*, 1995, **28**, 8722–8728.

5 G. Moad, D. H. Solomon and G. Moad, *The Chemistry of Radical Polymerization*, Elsevier, Amsterdam; Boston, 2006, and references cited therein.

6 J. Nicolas, Y. Guillaneuf, C. Lefay, D. Bertin, D. Gigmes and B. Charleux, Nitroxide-Mediated Polymerization, *Prog. Polym. Sci.*, 2013, **38**, 63–235.

7 D. Gigmes and S. R. A. Marque, *Encyclopedia of Radicals in Chemistry, Biology, and Materials*, ed. C. Chatgilialoglu and A. Studer, Wiley, Chichester, U.K., 2012, vol. 4, pp. 1813–1850.

8 X. Pan, M. A. Tasdelen, J. Laun, T. Junkers, Y. Yagci and K. Matyjaszewski, Photomediated Controlled Radical Polymerization, *Prog. Polym. Sci.*, 2016, **62**, 73–125.

9 *Nitroxide Mediated Polymerization: From Fundamentals to Applications in Materials Science*, RSC polymer chemistry series, ed. D. Gigmes, Royal Society of Chemistry, Cambridge, 2016.

10 M. V. Edeleva, E. G. Bagryanskaya and S. R. A. Marque, Imidazoline and Imidazolidine Nitroxides as Controlling Agents in Nitroxide-Mediated Pseudoliving Radical Polymerization, *Russ. Chem. Rev.*, 2018, **87**(4), 328–349.

11 M. Destarac, Controlled Radical Polymerization: Industrial Stakes, Obstacles and Achievements, *Macromol. React. Eng.*, 2010, **4**, 165–179.

12 E. H. H. Wong, T. Junkers and C. Barner-Kowollik, Nitrones in Synthetic Polymer Chemistry, *Polym. Chem.*, 2011, **2**, 1008–1010.

13 Y. Guillaneuf, D. Bertin, D. Gigmes, D. L. Versace, J. Lalevee and J. P. Fouassier, Toward Nitroxide-Mediated Photopolymerization, *Macromolecules*, 2010, **43**, 2204–2212.

14 D. L. Versace, J. Lalevee, J. P. Fouassier, D. Gigmes, Y. Guillaneuf and D. Bertin, Photosensitized Alkoxyamines as Bicomponent Radical Photoinitiators, *J. Polym. Sci., Part A: Polym. Chem.*, 2010, **48**, 2910–2915.

15 E. Yoshida, Nitroxide-Mediated Photo-Living Radical Polymerization of Methyl Methacrylate in Solution, *Colloid Polym. Sci.*, 2010, **288**, 1639–1643.

16 G. Audran, E. Bagryanskaya, M. Edeleva, S. R. A. Marque, D. Parkhomenko, E. Tretyakov and S. Zhivetyeva, Coordination-Initiated Nitroxide-Mediated Polymerization (CI-NMP), *Aust. J. Chem.*, 2018, **71**, 334–340.

17 J. O. Zoppe, N. C. Ataman, P. Mocny, J. Wang, J. Moraes and H. Klok, Surface-Initiated Controlled Radical Polymerization: State-of-the-Art, Opportunities, and Challenges in Surface and Interface Engineering with Polymer Brushes, *Chem. Rev.*, 2017, **117**, 1105–1318.

18 G. Audran, E. Bagryanskaya, I. Bagryanskaya, P. Brémond, M. Edeleva, S. R. A. Marque, D. Parkhomenko, O. Yu. Rogozhnikova, V. M. Tormyshev, E. V. Tretyakov, D. V. Trukhin and S. I. Zhivetyeva, Trityl-Based Alkoxyamines as NMP Controllers and Spin-Labels, *Polym. Chem.*, 2016, **7**, 6490–6499.

19 M. V. Edeleva, S. R. A. Marque, O. Yu. Rogozhnikova, V. M. Tormyshev, T. I. Troitskaya and E. G. Bagryanskaya, Radical Polymerization of Radical-Labeled Monomers: The Triarylmethyl-Based Radical Monomer as an Example, *J. Polym. Sci., Part A: Polym. Chem.*, 2018, **56**, 2656–2664.

20 O. Guselnikova, S. R. A. Marque, E. Tretyakov, D. Mares, V. Jerabek, G. Audran, J.-P. Joly, M. Trusova, V. Švorčik, O. Lyutakov and P. Postnikov, Unprecedented Plasmon-Induced Nitroxide-Mediated Polymerization (PI-NMP): A Method for Preparation of Functional Surfaces, *J. Mater. Chem. A*, 2019, **7**(20), 12414–12419.

21 C. Yuan, M. Z. Rong, M. Q. Zhang, Z. P. Zhang and Y. C. Yuan, Self-Healing of Polymers via Synchronous Covalent Bond Fission/Radical Recombination, *Chem. Mater.*, 2011, **23**, 5076–5081.

22 Z. P. Zhang, M. Z. Rong, M. Q. Zhang and C. Yuan, Alkoxyamine with Reduced Homolysis Temperature and Its

 This journal is © the Partner Organisations 2020

Open Access Article. Published on 30 July 2020. Downloaded on 7/29/2025 12:37:41 PM.
This article is licensed under a Creative Commons Attribution-NonCommercial 3.0 Unported Licence.

Application in Repeated Autonomous Self-Healing of Stiff Polymers, *Polym. Chem.*, 2013, **4**, 4648–4654.

23 B. Schulte, M. Tsotsalas, M. Becker, A. Studer and L. De Cola, Dynamic Microcrystal Assembly by Nitroxide Exchange Reactions, *Angew. Chem., Int. Ed.*, 2010, **49**, 6881–6884.

24 L. Charles, C. Laure, J.-F. Lutz and R. K. Roy, MS/MS Sequencing of Digitally Encoded Poly(alkoxyamine Amide) s, *Macromolecules*, 2015, **48**, 4319–4328.

25 R. K. Roy, A. Meszynska, C. E. Laure, L. Charles, C. Verchin and J.-F. Lutz, Design and Synthesis of Digitally Encoded Polymers That Can Be Decoded and Erased, *Nat. Commun.*, 2015, **6**, 1–8.

26 G. Cavallo, A. Al Ouahabi, L. Oswald, L. Charles and J.-F. Lutz, Orthogonal Synthesis of "Easy-to-Read" Information-Containing Polymers Using Phosphoramidite and Radical Coupling Steps, *J. Am. Chem. Soc.*, 2016, **138**, 9417–9420.

27 G. Audran, P. Brémond, J.-M. Franconi, S. R. A. Marque, P. Massot, P. Mellet, E. Parzy and E. Thiaudière, Alkoxyamines: A New Family of pro-Drugs against Cancer. Concept for Theranostics, *Org. Biomol. Chem.*, 2014, **12**, 719–723.

28 D. Moncelet, P. Voisin, N. Koonjoo, V. Bouchaud, P. Massot, E. Parzy, G. Audran, J.-M. Franconi, E. Thiaudière, S. R. A. Marque, P. Brémond and P. Mellet, Alkoxyamines: Toward a New Family of Theranostic Agents against Cancer, *Mol. Pharmaceutics*, 2014, **11**, 2412–2419.

29 N. A. Popova, G. M. Sysoeva, V. P. Nicolin, V. I. Kaledin, E. V. Tretyakov, M. V. Edeleva, S. M. Balakhnin, E. L. Louschnikova, G. Audran and S. Mark, Comparative Study of Toxicity of Alkoxyamines In Vitro and In Vivo, *Bull. Exp. Biol. Med.*, 2017, **164**(1), 49–53.

30 T. Yamasaki, D. Buric, Ch. Chacon, G. Audran, D. Braguer, S. R. A. Marque, M. Carré and P. Brémond, Chemical Modifications of Imidazole-Containing Alkoxyamines Increase C–ON Bond Homolysis Rate: Effects on Their Cytotoxic Properties in Glioblastoma Cells, *Bioorg. Med. Chem.*, 2019, **27**, 1942–1951.

31 J. Wang and J. Yi, Cancer Cell Killing via ROS: To Increase or Decrease, That Is the Question, *Cancer Biol. Ther.*, 2008, **7**, 1875–1884.

32 P. Brémond and S. R. A. Marque, First Proton Triggered C–ON Bond Homolysis in Alkoxyamines, *Chem. Commun.*, 2011, **47**(14), 4291–4293.

33 P. Brémond, A. Koïta, S. R. A. Marque, V. Pesce, V. Roubaud and D. Siri, Chemically Triggered C–ON Bond Homolysis of Alkoxyamines. Quaternization of the Alkyl Fragment, *Org. Lett.*, 2012, **14**(1), 358–361.

34 G. Audran, L. Bosco, P. Brémond, S. R. A. Marque, V. Roubaud and D. Siri, Chemically Triggered C–ON Bond Homolysis of Alkoxyamines. 8. Quaternization and Steric Effects, *J. Org. Chem.*, 2013, **78**, 9914–9920.

35 G. Audran, E. Bagryanskaya, I. Bagryanskaya, P. Brémond, M. Edeleva, S. R. A. Marque, D. Parkhomenko, E. Tretyakov and S. Zhivetyeva, C–ON Bond Homolysis of Alkoxyamines Triggered by Paramagnetic Copper(II) Salts, *Inorg. Chem. Front.*, 2016, **3**(11), 1464–1472.

36 G. Audran, E. Bagryanskaya, I. Bagryanskaya, M. Edeleva, S. R. A. Marque, D. Parkhomenko, E. Tretyakov and S. Zhivetyeva, Zinc(II) Hexafluoroacetylacetonate Complexes of Alkoxyamines: NMR and Kinetic Investigations. First Step for a New Way to Prepare Hybrid Materials, *ChemistrySelect*, 2017, **2**, 3584–3593.

37 M. V. Edeleva, I. A. Kirilyuk, I. F. Zhurko, D. A. Parkhomenko, Y. P. Tsentalovich and E. G. Bagryanskaya, pH-Sensitive C–ON Bond Homolysis of Alkoxyamines of Imidazoline Series with Multiple Ionizable Groups As an Approach for Control of Nitroxide Mediated Polymerization, *J. Org. Chem.*, 2011, **76**, 5558–5573.

38 G. Audran, E. Bagryanskaya, I. Bagryanskaya, M. Edeleva, P. Klina, S. R. A. Marque, D. Parkhomenko, E. Tretyakov and S. Zhivetyeva, The Effect of the Oxophilic Tb(III) Cation on C ON Bond Homolysis in Alkoxyamines, *Inorg. Chem. Commun.*, 2018, **91**, 5–7.

39 G. Audran, P. Brémond and S. R. A. Marque, Labile Alkoxyamines: Past, Present, and Future, *Chem. Commun.*, 2014, **50**(59), 7921–7928.

40 G. Audran, L. Bosco, P. Brémond, N. Jugniot, S. R. A. Marque, P. Massot, P. Mellet, T. Moussounda Moussounda Koumba, E. Parzy, A. Rivot, E. Thiaudière, P. Voisin, C. Wedl and T. Yamasaki, Enzymatic Triggering of C–ON Bond Homolysis of Alkoxyamines, *Org. Chem. Front.*, 2019, **6**, 3663–3672.

41 S. Edvinsson, S. Johansson and A. Larsson, An Efficient Procedure for the Synthesis of Formylacetic Esters, *Tetrahedron Lett.*, 2012, **53**, 6819–6821.

42 J. H. A. Babler, A Facile Route to Glyoxal Mono(diethyl Acetal): A Versatile Synthon for Preparation of A,β-Unsaturated Aldehydes, *Synth. Commun.*, 1987, **17**, 77–84.

43 K. Matyjaszewski, B. E. Woodworth, X. Zhang, S. G. Gaynor and Z. Metzner, Simple and Efficient Synthesis of Various Alkoxyamines for Stable Free Radical Polymerization, *Macromolecules*, 1998, **31**, 5955–5957.

44 J. M. Álvarez-Calero, Z. D. Jorge and G. M. Massanet, $TiCl_4$/Et_3 N-Mediated Condensation of Acetate and Formate Esters: Direct Access to β-Alkoxy- and β-Aryloxyacrylates, *Org. Lett.*, 2016, **18**, 6344–6347.

45 P. Nkolo, G. Audran, R. Bikanga, P. Brémond, S. R. A. Marque and V. Roubaud, C–ON Bond Homolysis of Alkoxyamines: When Too High Polarity Is Detrimental, *Org. Biomol. Chem.*, 2017, **15**, 6167–6176.

46 E. G. Bagryanskaya and S. R. A. Marque, Kinetic Aspects of Nitroxide Mediated Polymerization, in *Polymer Chemistry Series*, ed. D. Gigmes, Royal Society of Chemistry, Cambridge, 2015, pp. 45–113.

47 D. Bertin, D. Gigmes, S. R. A. Marque and P. Tordo, Polar, Steric, and Stabilization Effects in Alkoxyamines C–ON Bond Homolysis: A Multiparameter Analysis, *Macromolecules*, 2005, **38**(7), 2638–2650.

Open Access Article. Published on 30 July 2020. Downloaded on 7/29/2025 12:37:41 PM.
This article is licensed under a Creative Commons Attribution-NonCommercial 3.0 Unported Licence.

48 E. Beaudoin, D. Bertin, D. Gigmes, S. R. A. Marque, D. Siri and P. Tordo, Alkoxyamine C–ON Bond Homolysis: Stereoelectronic Effects, *Eur. J. Org. Chem.*, 2006, 1755–1768.
49 G. Audran, P. Brémond, S. R. A. Marque and G. Obame, Chemically Triggered C–ON Bond Homolysis of Alkoxyamines. Part 4: Solvent Effect, *Polym. Chem.*, 2012, **3**, 2901–2908.
50 G. Audran, P. Brémond, S. R. A. Marque and G. Obame, Chemically Triggered C–ON Bond Homolysis of Alkoxyamines. 5. Cybotactic Effect, *J. Org. Chem.*, 2012, **77**(21), 9634–9640.
51 K. A. Connors, *Chemical Kinetics: The Study of Reaction Rates in Solution*, Wiley-VCH, Nachdr., New York, NJ, 1990.
52 S. Marque, C. Le Mercier, P. Tordo and H. Fischer, Factors Influencing the C–O–Bond Homolysis of Trialkylhydroxylamines, *Macromolecules*, 2000, **33**(12), 4403–4410.
53 I. V. Alabugin, *Stereoelectronic Effects: A Bridge between Structure and Reactivity*, Wiley, Chichester, West Sussex, UK; Hoboken, NJ, USA, 2016.
54 A. Gaudel-Siri, D. Siri and P. Tordo, Homolysis of *N*-Alkoxyamines: A Computational Study, *ChemPhysChem*, 2006, **7**, 430–438.
55 G. Audran, R. Bikanga, P. Brémond, M. Edeleva, S. R. A. Marque, P. Nkolo and V. Roubaud, How Intramolecular Hydrogen Bonding (IHB) Controls the C–ON Bond Homolysis in Alkoxyamines, *Org. Biomol. Chem.*, 2017, **15**, 8425–8439.
56 G. Audran, E. Bagryanskaya, I. Bagryanskaya, M. Edeleva, J.-P. Joly, S. R. A. Marque, A. Iurchenkova, P. Kaletina, S. Cherkasov, T. H. Tung, E. Tretyakov and S. Zhivetyeva, How Intramolecular Coordination Bonding (ICB) Controls the Homolysis of the C–ON Bond in Alkoxyamines, *RSC Adv.*, 2019, **9**, 2576–25789.

This journal is © the Partner Organisations 2020